Digest Journal of Nanomaterials and Biostructures Vol. 20, No. 4, October-December 2025, p. 1599-1608

Hydrothermal synthesis and surface characterization of ZnO prepared in different conditions

G. A. Fadhil [a, 1*], A. M. Zaki [b], N. A. Jaber [b]
[a] *College of Engineering, Al-Karkh University of Science, 10010 Baghdad, Iraq.*
[b] *College of Science, Al-Karkh University of Science, 10010 Baghdad, Iraq.*

Zinc oxide (ZnO) powders were prepared by using a hydrothermal process conducted at temperatures of 70° C and 90° C for a reaction time of 24 h and 48 h. The synthesis was performed in a locally fabricated hydrothermal unit that provides an economical method of acquiring ZnO structures. The surface and structural properties of the prepared powders were then studied using a combination of a number of techniques. The obtained powders displayed a crystalline hexagonal wurtzite phase, which was confirmed by the X-ray diffraction (XRD). The variation in the crystallite size and dislocation density was conditioned by the reaction temperature and process time, which means that the microstructure development was severely affected by the environment in which it was synthesized. Atomic force microscopy (AFM) combined with scanning electron microscopy (SEM) revealed that there were clear differences in particle uniformity and roughness over the parameters of preparation, and considered that thermal and temporal conditions had a direct influence on the growth and surface formation of the particles. Fourier transform infrared (FTIR) spectroscopy further confirmed the successful formation of ZnO through the identification of characteristic Zn–O stretching vibrations in all prepared samples. The collective results emphasize that careful adjustment of hydrothermal parameters can effectively tailor both structural and surface features of ZnO powders, which can subsequently be optimized for diverse technological fields such as gas sensing and optoelectronic devices.

(Received September 10, 2025; Accepted December 16, 2025)

Keywords: XRD, Hydrothermal, FTIR, Powder, Roughness

1. Introduction

Zinc oxide (ZnO) has received extensive scientific research for its properties that are suitable for optoelectronic and sensing applications [1–3]. Its most notable properties include a band gap of 3.37 eV [3], chemical stability, non-toxicity [4], relatively high optical transparency [5], electrical conductivity, and acceptable thermal resistance [6]. Structurally, ZnO has a hexagonal wurtzite structure. These properties make it a suitable choice for a variety of applications. They highlight the importance of having the ability to control them by changing the preparation conditions or the proportion of added elements. Providing this control over properties helps to improve or develop ZnO properties to suit the needs of the applications.

Scientific efforts have focused on developing methods to determine the morphology, size, and crystal quality of ZnO nanostructures [1, 7, 8]. Conventional routes such as sol–gel, vapor-phase transport, chemical vapor deposition (CVD), and sputtering have been widely explored, but

* Corresponding author: ghaiath.fadhil@kus.edu.iq
https://doi.org/10.15251/DJNB.2025.204.1599

many of them require high temperatures, vacuum systems, or expensive precursors, which limit scalability [7]. In contrast, the hydrothermal method has emerged as a particularly attractive alternative because it allows for the synthesis of highly crystalline ZnO nanostructures under relatively mild conditions—typically below 200 °C—using aqueous solutions [10]. This technique offers several advantages: simplicity, low cost, environmental friendliness, and the ability to precisely control particle size, aspect ratio, and crystallinity through reaction parameters adjustment such as temperature, precursor concentration, and reaction time [10,11].

In the hydrothermal process, zinc salts (e.g., $Zn(NO_3)_2$ or $Zn(CH_3COO)_2$) are reacted with alkaline agents (such as NaOH or NH_4OH) in an autoclave, where the temperature and pressure drive nucleation and crystal growth [10]. In hydrothermal synthesis, temperature is an issue. There is increased growth and crystal formation with an increase in temperature. This provides improved crystal quality and larger-sized particles. In addition, an increase in temperature increases the aggregation of the particles [10]. When the reaction is short-term, the particles of ZnO are smaller and contain more defects. The longer reaction times allow the particles to form shapes that have fewer defects and a higher quality of the crystal [10,11]. The quantity of starting material and the pH of the solution also make a significant impact on the size of the particles and their shape [7,10]. When these settings are altered, it is possible to shape ZnO nanostructures to suit us.

All this demonstrates that the optical properties of ZnO are altered by the hydrothermal conditions. The presence of missing oxygen atoms and extra spaces in the zinc metal affects the electrical conductivity, the intensity with which it shines/brightness and the way the zinc metal captures light within the visible spectrum. Then it is possible to eliminate or even add undesirable defects to achieve improved performance by the way to change the conditions of synthesis. As mentioned earlier, the shape of the surface and the orientation of the crystal is highly desirable towards the production of ZnO devices that can glow more efficiently and respond better on the surface [7]. Moreover, the ZnO nanocrystals prepared at reduced temperatures or shorter periods tend to exhibit a blue shift in the absorption edge, and this is due to quantum confinement effects [8,10]. This demonstrates that hydrothermal synthesis can adjust finely the optical bandgap of ZnO.

We aim to investigate the effect of hydrothermal conditions on the crystallinity and surface roughness of ZnO powders in this study. These powders were characterized using a combination of advanced techniques including X-ray Diffraction (XRD), atomic force microscopy (AFM), scanning electron microscopy (SEM) and Fourier transform infrared (FTIR) spectroscopy.

2. Experimental Section

Commercially available ZnO nanopowder that have an average particle size of 20–30 nm was the starting material. Sodium hydroxide (NaOH, pellets, Sigma-Aldrich, 98%), deionized distilled water, ethanol (99.7%), and acetone (99.7%) were used without further purification. Hydrochloric acid (HCl, 37%) and ethylene glycol (99.8%) were also employed for cleaning and processing steps. All chemicals were of analytical grade.

The hydrothermal process was carried out using a locally designed hydrothermal device, consisting of two main components: Thermal and Electrical control units (Fig. 1). The thermal unit is a stainless-steel crucible surrounded by heating coils [3000 W], capable of maintaining stable reaction temperatures. The Electrical control unit is a homemade control panel allowing precise voltage and temperature regulation, equipped with a thermal sensor and safety features. This device was fabricated locally and optimized for reactions up to 90 °C and pressures up to ~11 bar.

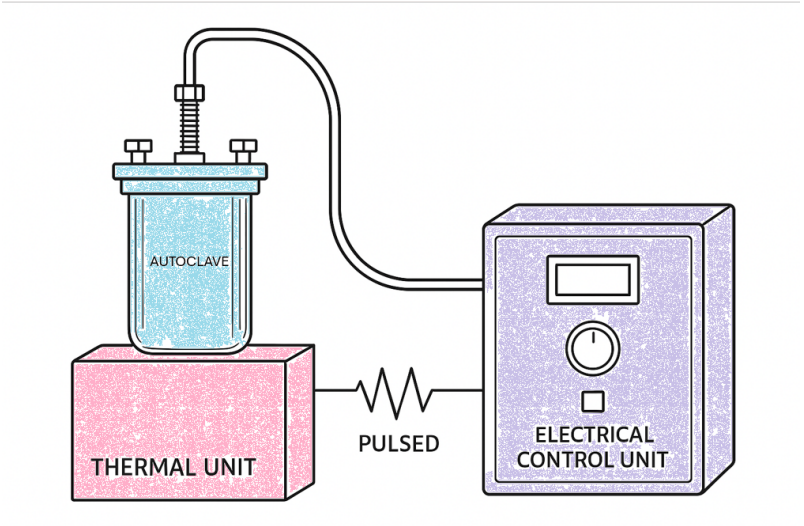

Fig. 1. A sketch of the locally designed hydrothermal device.

The following techniques were used to characterize the resulting ZnO powder. XRD was performed using a Shimadzu XRD-7000 with Cu Kα radiation (λ = 1.54 Å). The surface topography of the resulting powders was examined using an Angstrom Advanced AA3000 AFM. A Hitachi S-4160 field-emission SEM was used to image the powder surface. A PerkinElmer spectrometer equipped with an ATR accessory was the FTIR spectroscopy used to identify the functional groups and bonding properties.

ZnO nanopowder (1 g) was dispersed in 20 mL of NaOH aqueous solutions of varying concentrations (3 M and 6 M). The suspensions were magnetically stirred for 1 h. Then, they were transferred into Teflon-lined stainless-steel autoclaves (100 mL). The sealed autoclaves were placed inside the locally designed hydrothermal device and kept at two different temperatures (70 °C and 90 °C) for three different durations (24 h and 48 h). The products were washed several times with deionized water and ethanol after cooling to room temperature and until a neutral pH was reached. The powders were dried at 80 °C for 4 h, followed by annealing at 500 °C for 1 h to remove residual organic content.

3. Results and Discussion

The x-ray spectra of the hydrothermally treated ZnO powders for the samples prepared at 70 °C for 24 h and 48 h are shown in Fig. 2. The diffraction peaks in the 24h and 48h samples indicate a hexagonal wurtzite ZnO structure [JCPDS Card No. 36-1451] [12]. This confirms the phase purity of the prepared materials. No secondary phases or impurities such as Zn metal or $Zn(OH)_2$ were matched, indicating that the hydrothermal conditions successfully stabilized the ZnO crystalline phase. The diffraction peaks of the (002), (101) and (103) planes are clearly visible in both samples.

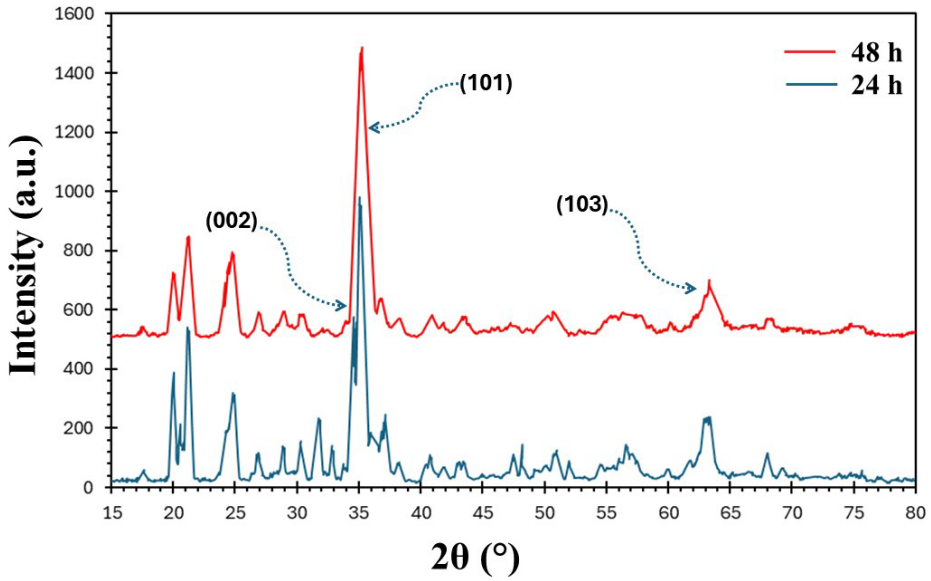

Fig. 2. XRD pattern of ZnO structures as-prepared for 24h and 48 h at 70 °C.

A comparison between the two samples shows a slight broadening of peaks with increasing reaction time from 24 h to 48 h. This broadening is associated with a reduction in crystallite size and an increase in lattice defects. Table 1 summarizes the structural parameters, including crystallite size [D], lattice strain [ε], and dislocation density [δ]. For the 70 °C series, the average crystallite size was calculated to reduce from ~19.0 nm to ~11.5 nm with the increased processing time from 24 h to 48 h, respectively. Similarly, the dislocation density increased significantly from 3.78×10^{15} to 8.17×10^{15} line/m², suggesting that extended hydrothermal treatment time promotes defect formation and structural distortion. The microstrain values remained in the order of 10^{-3}, which is typical for hydrothermally synthesized ZnO.

Table 1. The structural parameters for the 70 °C series.

	Lattice plane	2θ (Deg)	Crystallite size (nm)	Dislocation density, δ x10^{15}(line^2/m^2)
24 h	(002)	34.920	18.2869	2.99
	(101)	36.271	16.8987	3.50
	(103)	63.100	9.3312	11.4
48 h	(002)	34.990	10.0340	9.93
	(101)	36.780	9.1701	11.8
	(103)	62.670	10.3065	9.41

These results indicate that prolonging the hydrothermal treatment at moderate temperature (70 °C) does not improve crystallinity but instead leads to fragmentation and defect accumulation, which may later influence the surface morphology and roughness observed in SEM and AFM analysis.

XRD patterns of ZnO powders synthesized hydrothermally at 90 °C for 24 h and 48 h are shown in Fig. 3. The diffraction peaks indicate the hexagonal wurtzite ZnO structure [JCPDS card No. 36-1451], and no impurity phases such as metallic Zn or $Zn(OH)_2$ were observed, confirming the phase purity of the products. The main reflections were identified at the (100), (002), (101), (012), (110) and (103) planes. For the 48 h samples, the peaks are relatively broader and slightly less intense compared to the 24 h samples. This indicates a decrease in crystallite size and an increase in the density of lattice defects.

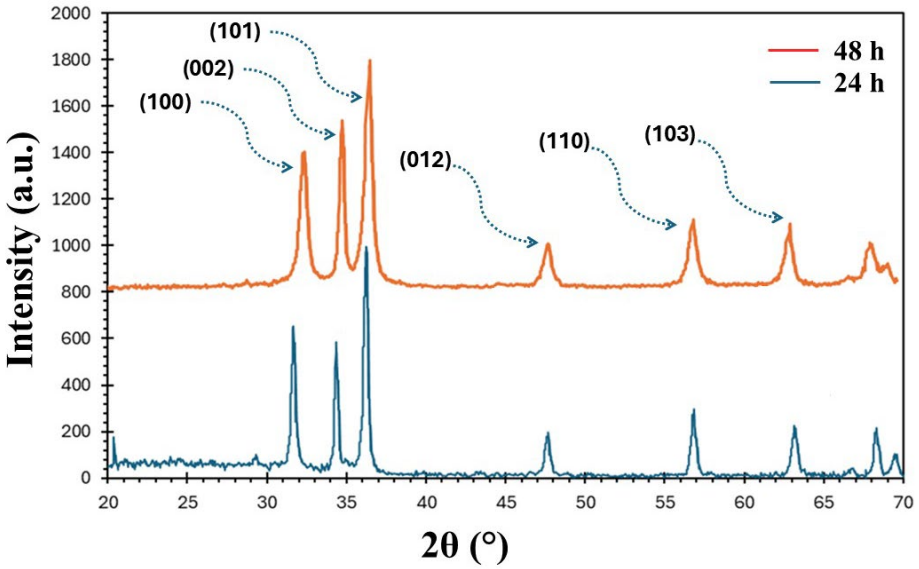

Fig. 3. XRD patterns of ZnO prepared at 90 °C for 24 h and 48 h.

The calculated average crystallite size decreased from about 26–32 nm (24 h) to about 12–20 nm (48 h). In contrast, the dislocation density increased from approximately 1.4×10^{15} line/m² for the 24 h sample to about 5.0×10^{15} line/m² for the 48 h sample, as summarized in Tables 2 and 3. These results confirm that extending the reaction time at 90 °C leads to fragmentation of crystallites and accumulation of structural defects.

Table 2. Structural parameters of ZnO samples prepared at 90 °C for 24 h.

Lattice plane	2θ (Deg)	Crystallite size (nm)	Dislocation density, δ x1015(line2/m2)
(100)	31.728	26.195	1.45
(002)	34.389	32.64	0.93
(101)	36.211	26.68	1.40
(012)	47.490	25.54	1.53
(110)	56.566	29.30	1.16
(103)	62.838	29.342	1.18
(112)	67.930	36.08	0.76

Table 3. Structural parameters of ZnO samples prepared at 90 °C for 48 h.

Lattice plane	2θ (Deg)	Crystallite size (nm)	Dislocation density, δ x1015(line2/m2)
(100)	31.920	13.6556	5.36
(002)	34.570	19.8420	2.53
(101)	36.390	14.1173	5.01
(102)	47.670	14.0809	5.04
(110)	56.700	14.0079	5.09
(103)	62.970	14.8721	4.52
(112)	68.060	12.97	5.94

The results confirm that increasing the temperature to 90 °C promoted faster growth compared with 70 °C, but a longer reaction time still resulted in higher defect density rather than further improvement in crystallinity.

The surface morphology of the ZnO powders was profiled using AFM. 3D images (shown in Fig. 4) provide information about the surface topography, revealing that the surface roughness increased with longer reaction time from 24 h to 48 h. The change in roughness is in agreement with the crystallite size reduction and the higher defect density observed in the XRD analysis (Tables 1, 2 & 3).

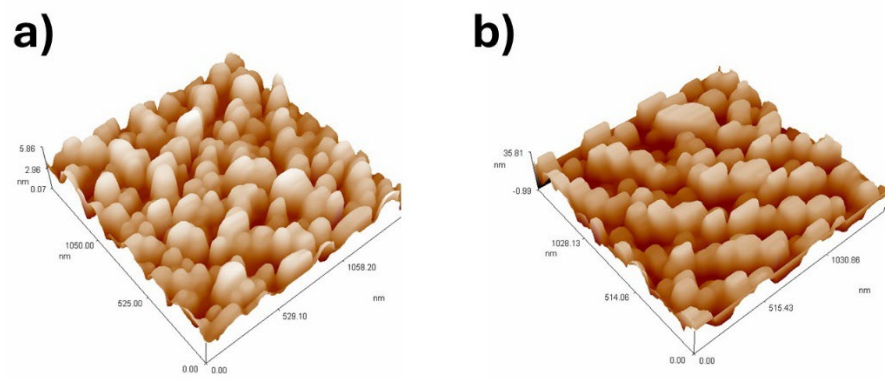

Fig. 4. 3D AFM images of ZnO prepared at 70 °C for (a) 24 h and (b) 48 h.

The 3D AFM images show the surface topography of the ZnO samples prepared at 90 °C (Fig. 5). The images reveal differences in surface roughness between the samples prepared for 24 h and 48 h. The roughness increased with longer reaction time, consistent with the reduction in crystallite size and the higher density of dislocations observed in the XRD results.

The surface morphology of ZnO samples prepared by the hydrothermal method was investigated using SEM. The SEM images are shown in Fig. 6 for the samples prepared at 70 °C with reaction times of 24 h and 48 h.

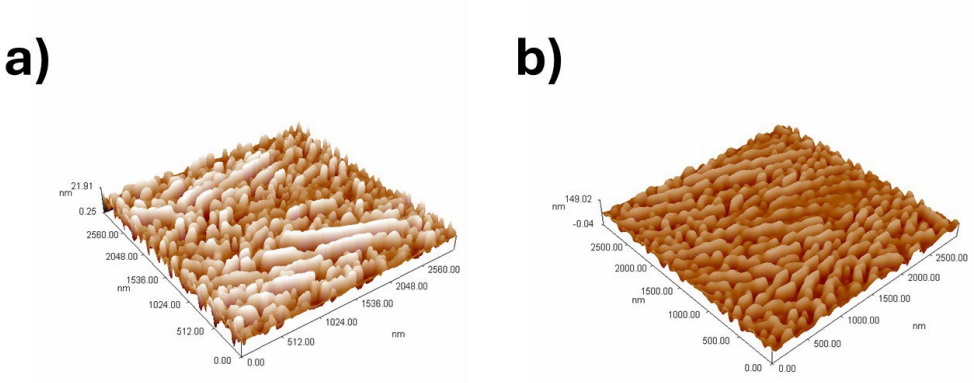

Fig. 5. 3D AFM image of ZnO prepared at 90 °C for (a) 24 h and (b) 48 h.

For the 24 h sample, the surface appeared relatively uniform with plate-like features and grains in the sub-micrometer range. The 48h sample appeared to have more irregular and aggregated structures. These reflect the influence of extended reaction time on the growth process. These morphological variations are consistent with the changes in crystallite size and defect density revealed by XRD and the roughness values observed by AFM.

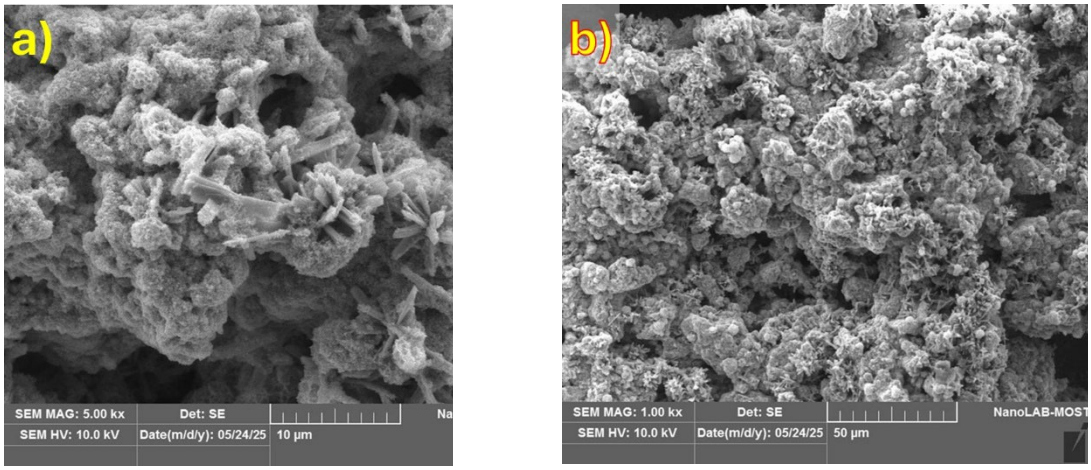

Fig. 6. SEM image of ZnO prepared at 70 °C for (a) 24 h and (b) 48 h.

For ZnO samples prepared at 90 °C the 24 h sample, the micrographs revealed elongated plate-like structures with relatively smooth surfaces (Fig. 7a). This indicates a more ordered growth at shorter reaction time. By contrast, the 48 h sample exhibited more compact and aggregated features, with noticeable variations in shape and size (Fig. 7b). These changes reflect the influence of prolonged reaction time on the surface development of ZnO. The observed morphological differences are consistent with the XRD and AFM results, where extended reaction time led to reduced crystallite size, higher defect density, and increased surface roughness.

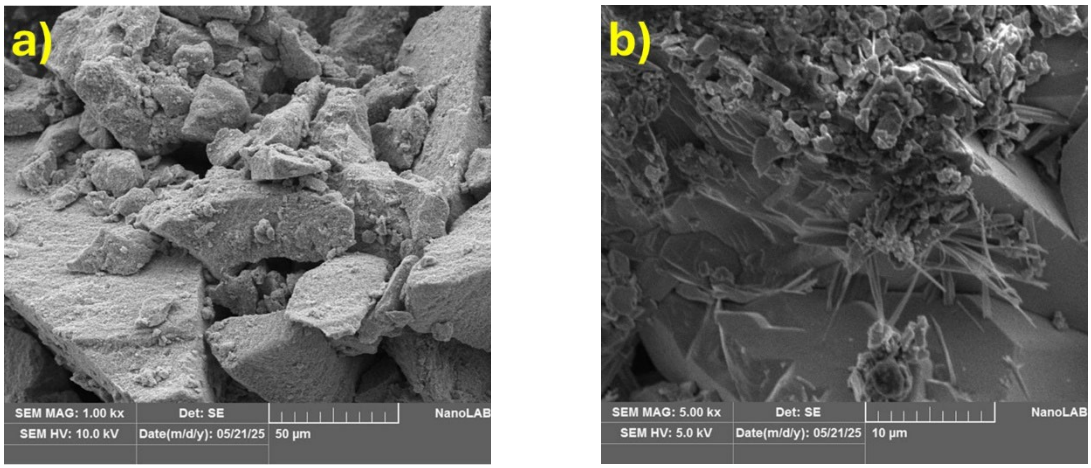

Fig. 7. SEM image of ZnO prepared at 90 °C for (a) 24 h and (b) 48 h.

The FTIR spectra of ZnO samples manufactured at 70 °C and 90 °C are presented in Fig. 8. A pronounced absorption band centered near 3400 cm^{-1} is observed, corresponding to O–H stretching vibrations arising from surface hydroxyl groups and adsorbed water molecules. The distinct peaks at approximately 1539 and 1419 cm^{-1} are associated with C–O stretching modes, which are likely due to carbonate species originating from atmospheric CO_2 adsorption. Absorption bands visible in the 1000–850 cm^{-1} range are attributed to Zn–O stretching vibrations, confirming the formation of ZnO successfully. In addition, the low-frequency bands detected between 711 and 553 cm^{-1} are characteristic of Zn–O lattice vibrations in the wurtzite crystal structure, further confirming the crystalline nature of the prepared samples.

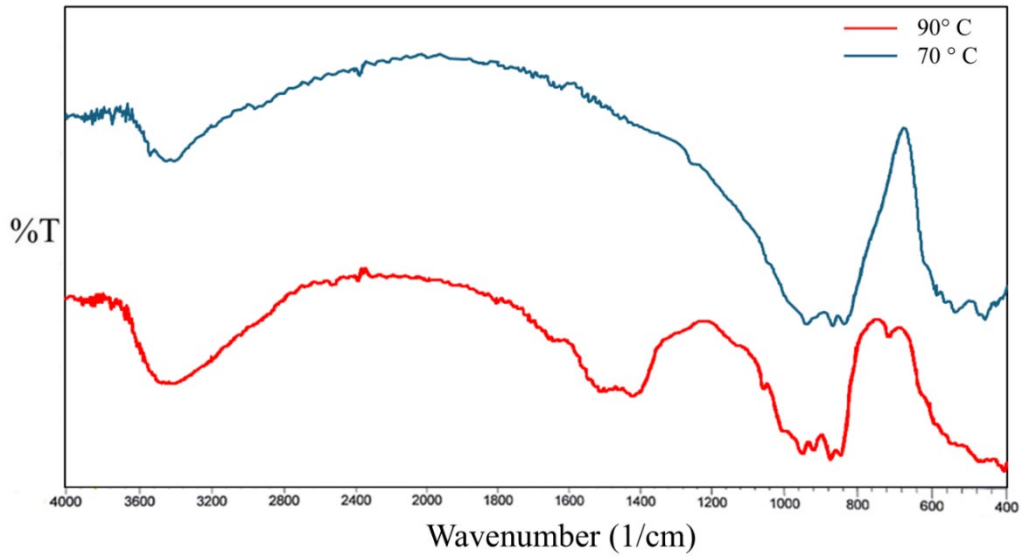

Fig. 8. FTIR spectrum of ZnO powders prepared at 24h.

Hydrothermal synthesis at 90 °C improved ZnO crystallinity compared to 70 °C, but extended reaction time promoted fragmentation, increased defect density, and higher surface roughness rather than further enhancement. Similar time-dependent defect generation has been recently reported in ZnO nanostructures synthesized under mild hydrothermal conditions [13, 14]. The observed correlation between crystallite refinement, dislocation density, and roughness evolution is also consistent with recent AFM and SEM studies of hydrothermally grown ZnO films [15]. Meanwhile, the preservation of Zn–O vibrational modes in the FTIR spectra confirms that the wurtzite structure remains stable, in agreement with recent FTIR investigations on low-temperature ZnO synthesis [16].

These results underline the critical balance between growth and defect accumulation during hydrothermal processing and suggest that simply prolonging synthesis time is not beneficial for improving structural quality. Recent studies highlight that controlling defect chemistry via surfactants, mineralizers, or pH regulation can significantly improve crystal quality and morphology [17,18]. Building on these insights, future work should integrate such strategies and directly correlate defect density with functional performance in optoelectronic and photocatalytic applications, where surface roughness and defect states strongly dictate device efficiency.

4. Conclusions

The present work examined how variations in hydrothermal conditions affect the crystallinity, morphology, and vibrational response of ZnO powders. It was observed that increasing the reaction temperature to 90 °C promoted faster crystal growth and yielded powders with a noticeably higher degree of crystallinity when compared with those synthesized at 70 °C. However, when the reaction at 90 °C was prolonged, partial fragmentation of the crystals appeared, accompanied by a rise in defect density, a reduction in crystallite size, and enhanced surface roughness. These findings illustrate that the hydrothermal route can be tuned to produce ZnO with specific structural and morphological characteristics, as verified by the clear Zn–O stretching bands of the wurtzite phase in the FTIR spectra.

Overall, the results confirm that adjusting the synthesis parameters directly governs the resulting microstructure and surface texture. Understanding and optimizing this interplay between composition, crystal arrangement, and processing conditions allow for the design of ZnO powders tailored for advanced applications such as optoelectronic and surface-engineered systems.

Availability of Data and Materials

The datasets used and analyzed during the current study are available from the corresponding author on reasonable request.

Author Contributions

G. Fadhil, A.M. Zaki and N. A. Jaber designed the research study. All authors performed the research. All authors participated in the analysis of the data. G. Fadhil drafted the manuscript. All authors contributed to critical revision of the manuscript for important intellectual content. All authors read and approved the final manuscript. All authors have participated sufficiently in the work and agreed to be accountable for all aspects of the work.

Acknowledgment

We would like to express our gratitude to all those who helped us during the writing of this manuscript. Thanks to all the peer reviewers for their opinions and suggestions.

Funding

This research received no external funding.

Conflict of Interest

The authors declare no conflict of interest.

Reference

[1] Ü. Özgür, Y. I. Alivov, C. Liu, Journal of Applied Physics 98(4), 041301(2005). https://doi.org/10.1063/1.1992666
[2] Shahzad, S., Javed, S., & Usman, M. (2021). A Review on Synthesis and Optoelectronic Applications of Nanostructured ZnO. Frontiers in Materials, 8. https://doi.org/10.3389/fmats.2021.613825
[3] D. C. Look, Materials Science and Engineering: B 80(1-3), 383–387(2001). https://doi.org/10.1016/S0921-5107(00)00604-8
[4] B. H. Yao, Y. F. Chen, M. S. Wu, Applied Physics Letters 81(5), 757–759(2002). https://doi.org/10.1063/1.1493660
[5] Logothetidis, S., Laskarakis, A., Kassavetis, S., Lousinian, S., Gravalidis, C., & Kiriakidis, G., Thin Solid Films, 516(7), 1345–1349 (2008). https://doi.org/10.1016/j.tsf.2007.03.171
[6] T. A. A. Hassan, A. Q. Tuama, G. A. Fadhil, Applied and Technological Sciences 12, 239–246(2024). https://doi.org/10.47832/MinarCongress12-22
[7] Z. L. Wang, Journal of Physics: Condensed Matter 16(25), R829–R858 (2004). https://doi.org/10.1088/0953-8984/16/25/R01
[8] J. V. Barth, G. Costantini, K. Kern, Nature 437(7059), 671–679(2005). https://doi.org/10.1038/nature04166
[9] S. Bhattacharyya, A. Gedanken, The Journal of Physical Chemistry C 112(12), 4517–4523 (2008). https://doi.org/10.1021/jp7100978
[10] Donia, D. T., Bauer, E. M., Missori, M., Roselli, L., Cecchetti, D., Tagliatesta, P., Gontrani, L., & Carbone, M., 13(4), 733(2021). https://doi.org/10.3390/sym13040733
[11] Baruah, S., & Dutta, J., Science and Technology of Advanced Materials, 10(1), 013001(2009). https://doi.org/10.1088/1468-6996/10/1/013001
[12] JCPDS Card No. 36-1451: Zinc Oxide (hexagonal wurtzite structure). International Centre for Diffraction Data (ICDD), Pennsylvania, USA.

[13] Pramanik, S., Ghosh, T., Ghosh, M., De, S. C., & Kuiri, P. K., Advanced Science, Engineering and Medicine, 9(5), 414–419(2017). https://doi.org/10.1166/asem.2017.1992
[14] Samadi, M., Zirak, M., Naseri, A., Khorashadizade, E., & Moshfegh, A. Z., Thin Solid Films, 605, 2–19(2016) https://doi.org/10.1016/j.tsf.2015.12.064
[15] Krajian, H., Abdallah, B., Kakhia, M., & AlKafri, N., Microelectronics Reliability, 125, 114352(2021). https://doi.org/10.1016/j.microrel.2021.114352
[16] Farbod, M., & Jafarpoor, E., Ceramics International, 40(5), 6605–6610(2014). https://doi.org/10.1016/j.ceramint.2013.11.116
[17] Ayoub, I., Kumar, V., Abolhassani, R., Sehgal, R., Sharma, V., Sehgal, R., Swart, H. C., & Mishra, Y. K. Nanotechnology Reviews, 11(1), 575–619(2022). https://doi.org/10.1515/ntrev-2022-0035
[18] Wahab, R., Ansari, S. G., Kim, Y. S., Song, M., & Shin, H.-S.. Applied Surface Science, 255(9), 4891–4896(2009). https://doi.org/10.1016/j.apsusc.2008.12.037